Multi-Way MIMO Amplify-and-Forward Relay Networks With Zero-Forcing

Gayan Amarasuriya, Chintha Tellambura and Masoud Ardakani
Department of Electrical and Computer Engineering, University of Alberta, Edmonton, AB, Canada T6G 2V4
Email: {amarasur, chintha, ardakani}@ece.ualberta.ca

***Abstract*—A pair-wise transmit/receive zero-forcing (Tx/Rx ZF) transmission strategy is proposed and analyzed for multiple-input multiple-output (MIMO) amplify-and-forward (AF) multi-way relay networks (MWRNs). The performance of this system set-up is studied by deriving lower and upper bounds of the overall outage probability, the corresponding high signal-to-noise ratio outage approximations, and the achievable diversity-multiplexing trade-off. The proposed pair-wise Tx/Rx ZF transmission strategy possesses a lower implementation complexity as each source requires only the instantaneous respective source-to-relay channel knowledge. Moreover, our analysis provides valuable insights into practical MIMO AF MWRN implementation.**

I. Introduction

Two-way relay networks (TWRNs) are as twice spectral efficient as one-way relay networks (OWRNs) [1], and hence, are being studied as an efficient transmission strategy for next generation wireless standards. In particular, the multiple-input multiple-output (MIMO) technologies can further improve the performance of single-antenna TWRNs [2], [3]. Multi-way relay networks (MWRNs) are the natural generalization of TWRNs in which more than two sources exchange their messages by using intermediate relays. To this end, in this paper, the performance of MIMO amplify-and-forward (AF) MWRNs with pair-wise transmit/receiver zero-forcing (Tx/Rx ZF) transmission is studied.

Multi-way communication channels have been first studied more than three decades ago [4]. However, the practical significance of them has not been fully exploited until the emergence of modern cooperative relay communication research. In this context, the multi-way channel has been exploited with the aid of relays, and consequently, MWRNs recently emerged [5]–[8]. Specifically, in [2], the achievable symmetric rate of full-duplex MWRNs are studied for several relay processing strategies. However, in general, half-duplex MWRNs are preferred over full-duplex MWRNs as the practical implementation of the latter is significantly complicated. Reference [6] studies the achievable sum rate of AF MWRNs, where multiple single-antenna sources exchange their messages via a multiple-antenna relay by employing linear beamforming. However, one notable deficiency of [6] is that the number of antennas at the relay must exceed the participating number of sources, which would indeed become impractical for large networks. In particular, [7] circumvents the aforementioned deficiency of [6] by aligning messages from the same pair of sources by employing a proactive relay precoder design, which first avoids inter-pair interference and then utilizes intra-pair interference for symbol decoding via network coding. However, both [6] and [7] treat single-antenna sources only. Moreover, in [8], a pair-wise transmission strategy is studied for MWRNs by employing so-called functional decode-and-forward (FDC) relay processing. However, one key deficiency of FDF in [8] is that it can only treat binary signaling exchanged in single-antenna MWRNs.

Specifically, in this paper, a pair-wise Tx/Rx ZF based transmission strategy, which circumvents most of the deficiencies of [6]–[8], is proposed and analyzed for MIMO AF MWRNs. In particular, our transmission strategy enjoys two-fold benefits; (i) handles higher order modulation schemes as it employs AF relay processing, and (ii) treats MIMO-enabled terminals as it is based on Tx/Rx ZF. Consequently, the proposed scheme reaps both diversity and spatial multiplexing gains subjected to the fundamental diversity-multiplexing trade-off (DMT).

In this paper, we consider a half-duplex MIMO wireless network consisting of $M \geq 2$ sources and one relay. In this network, M sources exchange M independent symbol vectors in two consecutive multiple-access (MAC) and broadcast (BC) phases each having $M-1$ time-slots. In the MAC phase, the ith and $(i+1)$th pair of sources, where $i \in \{1, \cdots, M-1\}$, transmit to the relay by employing transmit-ZF precoding, while the relay receives a superimposed-signal without using a specific receiver reconstruction filtering. This pair-wise MAC transmission takes place until the completion of the last pair's transmission. In the BC phase, relay performs a simple AF operation for each superimposed-signal received during the MAC phase by employing a specific gain, which is designed to constraint the long-term total transmission power at the relay. Then the relay broadcasts these $M-1$ signals in $M-1$ consecutive time-slots in the BC phase, where all the M sources receive these amplified superimposed-signals by employing their corresponding receive-ZF reconstruction filters. Consequently, each source now has $M-1$ independent signals from which the information bearing signal vectors belonging to the remaining $M-1$ sources can readily be decoded by using back-propagated successive interference cancellation.

In this work, the basis performance metrics of the aforementioned system set-up are quantified to obtain valuable insights into practical MIMO MWRN implementation. To this end, the lower and upper bounds of the overall outage probability, the corresponding high signal-to-noise ratio (SNR) outage approximations, and the fundamental DMT are derived in closed-form. Moreover, useful numerical results are presented to further validate the insights provided by our analysis.

It is worth noticing that our pair-wise Tx/Rx ZF strategy promises simple practical implementation as each source requires only the corresponding source-to-relay channel knowl-

978-1-4673-0921-9/12/$31.00 ©2012 IEEE

edge as opposed to the global CSI requirement, as well as the relay only requires the long-term channel statistics.

Notations: $\mathbf{Z}^H$, $[\mathbf{Z}]_{k,l}$, and $\lambda_k(\mathbf{Z})$ denote the Hermitian-transpose, the (k,l)th diagonal element and the kth eigenvalue of the matrix, $\mathbf{Z}$, respectively. $\mathcal{E}_\Lambda\{z\}$ is the expected value of z over Λ, and the operator $\otimes$ denotes the Kronecker product. $\mathbf{I}_M$ and $\mathbf{O}_{M\times N}$ are the $M\times M$ Identity matrix and $M\times N$ matrix of all zeros, respectively. $f(x)=o\left(g(x)\right)$, $g(x)>0$ states that $f(x)/g(x)\rightarrow 0$ as $x\rightarrow 0$.

II. System model

We consider a MIMO AF MWRN consisting of M sources (S_m) for $m\in\{1,\cdots,M\}$, and one relay node (R), where each of them operates in half-duplex mode. The mth source and the relay are equipped with N_m and N_R antennas respectively[1]. All the channel amplitudes are assumed to be independently distributed frequency-flat Rayleigh fading. The direct channel between S_i and S_j for $i\neq j$ is assumed to be unavailable due to heavy path-loss and shadowing [1].

In this MWRN, all M sources exchange their information-bearing vectors, $\mathbf{x}_m$, satisfying $\mathcal{E}\left[\mathbf{x}_m\mathbf{x}_m^H\right]=\mathbf{I}_{N_m}$ for $m\in\{1,\cdots,M\}$, each other in two consecutive MAC and BC transmission phases each of them having $M-1$ time-slots. In the ith time-slot of the MAC phase, the pair of sources, S_i and S_{i+1}, where $i\in\{1,\cdots,M-1\}$, transmit $\mathbf{x}_i$ and $\mathbf{x}_{i+1}$ simultaneously to R by employing transmit-ZF precoding. The received superimposed-signal vector at R in the ith time-slot of MAC phase is thus given by

$$\mathbf{y}_R^{(i)}=g_i\mathbf{H}_{i,R}\mathbf{U}_i\mathbf{x}_i+g_{i+1}\mathbf{H}_{i+1,R}\mathbf{U}_{i+1}\mathbf{x}_{i+1}+\mathbf{n}_R^{(i)}, \quad (1)$$

where $\mathbf{H}_{i,R}\sim\mathcal{CN}_{N_R\times N_i}\left(\mathbf{0}_{N_R\times N_i},\mathbf{I}_{N_R}\otimes\mathbf{I}_{N_i}\right)$ is the channel matrix[2] from S_i to R, and $\mathbf{n}_R^{(i)}$ is the $N_R\times 1$ zero mean additive white Gaussian noise (AWGN) vector[3] at R in the ith time-slot of the MAC phase. Moreover, $\mathbf{U}_i$ is the transmit-ZF precoding matrix at S_i, and is given by [9]

$$\mathbf{U}_i=\mathbf{H}_{i,R}^H\left(\mathbf{H}_{i,R}\mathbf{H}_{i,R}^H\right)^{-1}\mathbf{\Pi}_i, \quad (2)$$

where $\mathbf{\Pi}_i$ is the $N_R\times N_i$ permutation matrix[4], which ensures only N_R data streams are transmitted by S_i for $i\in\{1,\cdots.M\}$. In (1), g_i is the power normalizing factor, which constraints the long-term total power at S_i, and is given by

$$g_i=\sqrt{\mathcal{P}_i/\mathrm{Tr}\left(\mathcal{E}\left[\mathbf{U}_i\mathbf{U}_i^H\right]\right)}=\sqrt{\mathcal{P}_i/\mathcal{T}_i}, \quad (3)$$

where $\mathcal{T}_i\triangleq\mathrm{Tr}\left(\mathcal{E}\left[\mathbf{U}_i\mathbf{U}_i^H\right]\right)=\frac{N_R}{N_i-N_R}$ [10] and $\mathcal{P}_i$ is the transmit power at S_i. The aforementioned MAC phase continues until the last pair of sources, S_{M-1} and S_M, complete their transmission, and consequently, R has now received M–1 pair-wise transmissions.

During the BC phase, R broadcasts the amplified version of the $M-1$ received signals back to all M sources in $M-1$ consecutive time-slots. In the jth time-slot of the BC phase, the received signal at the mth source is given by

$$\mathbf{y}_{S_m}^{(j)}=\mathbf{V}_m^{(j)}\Big(G_j\mathbf{H}_{R,i}^{(j)}\mathbf{y}_R^{(i)}+\mathbf{n}_m^{(j)}\Big),\ \text{for } j\in\{1,\cdots,M-1\}, (4)$$

where $G_j=\sqrt{\mathcal{P}_R/(g_j^2+g_{j+1}^2+\sigma_R^2)}$ is the power normalizing constant designed to constraint the long-term total power at R, P_R is the transmit power at R and $\mathbf{n}_m^{(j)}$ is the $N_m\times 1$ zero mean AWGN vector[5] at S_m for $m\in\{1,\cdots,M\}$. In (4), $\mathbf{V}_m^{(j)}$, $m\in\{1,\cdots,M\}$, is the receive-ZF matrix at S_m employed in the jth time-slot, and is given by [9]

$$\mathbf{V}_m^{(j)}=\left(\left(\mathbf{H}_{R,m}^{(j)}\right)^H\mathbf{H}_{R,m}^{(j)}\right)^{-1}\left(\mathbf{H}_{R,i}^{(j)}\right)^H,\ \text{for } j\in\{1,\cdots,M–1\}. (5)$$

In (4) and (5), $\mathbf{H}_{R,m}^{(j)}\sim\mathcal{CN}_{N_m\times N_R}\left(\mathbf{0}_{N_m\times N_R},\mathbf{I}_{N_m}\otimes\mathbf{I}_{N_R}\right)$ is the channel matrix[6] from R to S_m in the jth time-slot of the BC phase, and is assumed to be statistically independent for different $m\in\{1,\cdots,M\}$ and $j\in\{1,\cdots,M-1\}$.

By substituting (1) and (5) into (4), and then by employing successive interference cancellation[7] [1], the signal vector pertaining to the nth source, received at the mth source in the jth time-slot of the BC phase is derived as

$$\mathbf{Y}_{S_m}^{(j,n)}=G_j\left(g_n\mathbf{x}_n+\mathbf{n}_R^{(j)}\right)+\mathbf{V}_m^{(j)}\mathbf{n}_m^{(j)}, \quad (6)$$

where $k\in\{1,\cdots,N_R\}$, $j\in\{1,\cdots,M-1\}$, $m\in\{1,\cdots,M\}$, $n\in\{1,\cdots,M\}$, and $m\neq n$. Then the post-processing end-to-end signal-to-noise ratio (e2e SNR) of the kth data subchannel of $\mathbf{Y}_{S_m}^{(j,n)}$ in (6) can be derived as in (7). Furthermore, in (7), $\bar{\gamma}_{R,m}=P_R/\sigma_m^2$, $\bar{\gamma}_{j,R}=P_j/\sigma_R^2$, and $\bar{\gamma}_{n,R}=P_n/\sigma_R^2$[8].

Remark II.1: The SNR random variables, $[\gamma_{S_m^{(j,n)}}]_k$, for $k\in\{1,\cdots,N_R\}$ are statistically correlated for a given set of j, m, and n values as noise term in (6) is colored due to $\mathbf{V}_m^{(j)}$. However, the set of $[\gamma_{S_m^{(j,n)}}]_k$ belonging to different j, m and n values are statistically independent.

III. Performance Analysis

In this section, the basic performance metrics of the MIMO AF MWRN with pair-wise transmit/receive ZF are derived. In this context, the lower and upper bounds of the outage probability of an arbitrary source are first derived in closed-form, and then, used to derive the corresponding bounds of the overall outage probability. Moreover, the high SNR outage probability approximations and the DMT are derived to obtain valuable insights into practical MIMO MWRN designs.

[1]In the sequel, the constraint $\min\left(N_1,\cdots,N_M\right)>N_R$ is imposed to employ joint transmit and receiver ZF for the same antenna configuration. Consequently, the maximum number of end-to-end data subchannels from S_i to R is constrained to N_R.

[2]Here, $\mathbf{H}_{i,R}$ and $\mathbf{H}_{i',R}$ are independent for $i,i'\in\{1,\cdots,M\}$ and $i\neq i'$.

[3]The noise vector at R satisfies $\mathcal{E}\left(\mathbf{n}_R^{(i)}\left(\mathbf{n}_R^{(i)}\right)^H\right)=\mathbf{I}_{N_R}\sigma_R^2$.

[4]The permutation matrix, $\mathbf{\Pi}_i$, is constructed by horizontally concatenating a $N_R\times N_R$ permutation matrix and a $N_R\times(N_i–N_R)$ zero matrix, where $i\in\{1,\cdots,M\}$.

[5]The AWGN noise vector, $\mathbf{n}_m^{(j)}$, satisfies $\mathcal{E}\left(\mathbf{n}_m^{(j)}\left(\mathbf{n}_m^{(j)}\right)^H\right)=\mathbf{I}_{N_m}\sigma_m^2$ for $m\in\{1,\cdots,M\}$.

[6]$\mathbf{H}_{R,m}^{(j)}$ and $\mathbf{H}_{R,m'}^{(j')}$ are independent for $(j,j')\in\{1,\cdots,M-1\}$, $(m,m')\in\{1,\cdots,M\}$, $j\neq j'$ and $m\neq m'$.

[7]It is assumed that S_m knows its own information-bearing symbol vector, $\mathbf{x}_m$, CSI of $\mathbf{H}_{m,R}$, and G_j, which requires g_j, for $j\in\{1,\cdots,M-1\}$.

[8]It is worth noticing that the index pair (j,n) in (6) and (7) is used only to differentiate the sequence of symbol vectors received by a particular source in each time-slot of the BC phase from the remaining set of sources. Thus, each pair of (j,n) has a one-to-one correspondence, and hence, without loss of generality, the index n is removed herein for the sake of notational simplicity.

$$\left[\gamma_{S_m^{(j,n)}}\right]_k = \frac{\bar{\gamma}_{R,m}\bar{\gamma}_{n,R}\mathcal{T}_j\mathcal{T}_{j+1}\mathcal{T}_n^{-1}}{\bar{\gamma}_{R,m}\mathcal{T}_j\mathcal{T}_{j+1} + (\bar{\gamma}_{j,R}\mathcal{T}_{j+1} + \bar{\gamma}_{j+1,R}\mathcal{T}_j + \mathcal{T}_j\mathcal{T}_{j+1})\left[\left(\left(\mathbf{H}_{R,m}^{(j)}\right)^H \mathbf{H}_{R,m}^{(j)}\right)^{-1}\right]_{k,k}}, \tag{7}$$

A. The outage probability of an arbitrary source

In this subsection, the outage probability of the mth source for $m \in \{1, \cdots, M\}$ is derived. In our MWRN, the mth source receives $M-1$ symbol vectors pertaining to the remaining $M-1$ sources in the BC phase. In this context, the outage probability of a multi-subchannel system is governed by the performance of the weakest subchannel [11]. Thus, the outage probability of the mth source is defined as

$$P_{\text{out,m}} = \Pr\left(\min_{\substack{k\in\{1,\cdots,N_R\}\\ j\in\{1,\cdots,M-1\}}} \left[\gamma_{S_m^{(j)}}\right]_k \leq \gamma_{th}\right), \tag{8}$$

where γ_{th} is the threshold SNR[9]. The direct computation of (8) is mathematically intractable due to the correlation of $[\gamma_{S_m^{(j)}}]_k$ for $k \in \{1 \cdots N_R\}$ for a given j. Thus, simple lower and upper bounds of the outage probability are derived in closed-form.

1) Lower bound of $P_{\text{out,m}}$: The lower bound of the outage probability of the mth source can be derived as (see Appendix I for the proof)

$$P_{\text{out,m}}^{\text{lb}} = 1 - \prod_{j=1}^{M-1}\left(1 - F_{\gamma_{S_{m,\min}}^{(j),\text{ub}}}(\gamma_{th})\right), \tag{9}$$

where $F_{\gamma_{S_{m,\min}}^{(j),\text{ub}}}(x)$ is the CDF of $\gamma_{S_{m,\min}}^{(j),\text{ub}}$, and is given by

$$F_{\gamma_{S_{m,\min}}^{(j),\text{ub}}}(x) = \begin{cases} \frac{\gamma\left(N_m - N_R + 1, \frac{\mu_m^{(j)} x}{\eta_m^{(j)} - \zeta_m^{(j)} x}\right)}{\Gamma(N_m - N_R + 1)}, & 0 < x < \frac{\eta_m^{(j)}}{\zeta_m^{(j)}} \\ 1, & x \geq \frac{\eta_m^{(j)}}{\zeta_m^{(j)}}, \end{cases} \tag{10}$$

where $\mu_m^{(j)} = \bar{\gamma}_{j,R}\mathcal{T}_{j+1} + \bar{\gamma}_{j+1,R}\mathcal{T}_j + \mathcal{T}_j\mathcal{T}_{j+1}$, $\eta_m^{(j)} = \bar{\gamma}_{R,m}\bar{\gamma}_{n,R}\mathcal{T}_j\mathcal{T}_{j+1}\mathcal{T}_n^{-1}$, and $\zeta_m^{(j)} = \bar{\gamma}_{R,m}\mathcal{T}_j\mathcal{T}_{j+1}$, where $m \in \{1, \cdots, M\}$, and $j \in \{1, \cdots, M-1\}$.

2) Upper bound of $P_{\text{out,m}}$: The upper bound of the outage probability of the mth source can be derived as (see Appendix II for the proof)

$$P_{\text{out,m}}^{\text{ub}} = 1 - \prod_{j=1}^{M-1}\left(1 - F_{\gamma_{S_{m,\min}}^{(j),\text{lb}}}(\gamma_{th})\right), \tag{11}$$

where $F_{\gamma_{S_{m,\min}}^{(j),\text{lb}}}(x)$ is the cumulative distribution function (CDF) of $\gamma_{S_{m,\min}}^{(j),\text{lb}}$ and is given by

$$F_{\gamma_{S_{i,\min}}^{(j),\text{lb}}}(x) = \begin{cases} 1 - \frac{\det\left[\mathbf{Q}_m\left(\frac{\mu_m^{(j)} x}{\eta_m^{(j)} - \zeta_m^{(j)} x}\right)\right]}{\prod_{l=1}^{N_R}[\Gamma(N_i - l + 1)\Gamma(N_R - l + 1)]}, & 0 < x < \frac{\eta_m^{(j)}}{\zeta_m^{(j)}} \\ 1, & x \geq \frac{\eta_m^{(j)}}{\zeta_m^{(j)}}. \end{cases} \tag{12}$$

The (u, v)th element of $N_R \times N_R$ matrix, $\mathbf{Q}_m(x)$ in (12) is given by [12, Eq. (2.73)]

$$[\mathbf{Q}_m(x)]_{u,v} = \Gamma(N_m - N_R + u + v - 1, x). \tag{13}$$

[9]This threshold SNR, γ_{th}, is set to satisfy the minimum service-rate constraint; $\gamma_{th} = 2^{\mathcal{R}_{th}} - 1$, where $\mathcal{R}_{th}$ is the target rate [11].

B. Overall outage probability

The outage probability of a multi-source/multi-subchannel system is governed by the performance of the smallest subchannel of the weakest source. Thus, the overall outage probability of the MIMO AF MWRN is defined as the probability that the smallest subchannel of the weakest source falls bellow a preset threshold as follows:

$$P_{\text{out}} = \Pr\left(\min_{\substack{k\in\{1,\cdots,N_R\}, j\in\{1,\cdots,M-1\}\\ m\in\{1,\cdots,M\}}} \left[\gamma_{S_m^{(j)}}\right]_k \leq \gamma_{th}\right), \tag{14}$$

Again, the exact closed-form evaluation of (14) appears mathematically intractable, and hence, tight lower and upper bounds of the overall outage probability are derived.

1) Lower bound of the overall outage probability: The lower bound of the overall outage probability can be defined by using (38) as follows:

$$P_{\text{out}} \geq P_{\text{out}}^{\text{lb}} = \Pr\left(\min_{m\in\{1,\cdots,M\}} \gamma_{S_{m,\min}}^{\text{ub}} \leq \gamma_{th}\right), \tag{15}$$

where $\gamma_{S_{m,\min}}^{\text{lb}} = \min_{j\in\{1,\cdots,M-1\}}\left(\gamma_{S_{m,\min}}^{(j),\text{ub}}\right)$ is defined in (38). Next, $P_{\text{out}}^{\text{lb}}$ can be derived in closed-form by using (9) as

$$P_{\text{out}}^{\text{lb}} = 1 - \prod_{m=1}^{M}\prod_{j=1}^{M-1}\left(1 - F_{\gamma_{S_{m,\min}}^{(j),\text{ub}}}(\gamma_{th})\right), \tag{16}$$

where $F_{\gamma_{S_{m,\min}}^{(j),\text{ub}}}(x)$ is defined in (10).

2) Upper bound of the overall outage probability: The upper bound of the overall outage probability is defined by using (45) as follows:

$$P_{\text{out}} \leq P_{\text{out}}^{\text{ub}} = \Pr\left(\min_{m\in\{1,\cdots,M\}} \gamma_{S_{m,\min}}^{\text{lb}} \leq \gamma_{th}\right), \tag{17}$$

where $\gamma_{S_{m,\min}}^{\text{ub}} = \min_{j\in\{1,\cdots,M-1\}}\left(\gamma_{S_{m,\min}}^{(j),\text{lb}}\right)$ is defined in (45). Then, $P_{\text{out}}^{\text{ub}}$ is derived in closed-form by using (11) as

$$P_{\text{out}}^{\text{ub}} = 1 - \prod_{m=1}^{M}\prod_{j=1}^{M-1}\left(1 - F_{\gamma_{S_{m,\min}}^{(j),\text{lb}}}(\gamma_{th})\right), \tag{18}$$

where $F_{\gamma_{S_{m,\min}}^{(j),\text{lb}}}(x)$ is defined in (12).

C. Asymptotic outage probability at high SNRs

In this subsection, the asymptotically exact high SNR approximations for the lower and upper bound of the overall outage probability are derived.

1) High SNR approximation of the lower bound of P_{out}: The high SNR approximation for the lower bound of the outage probability of mth source can be derived as (see Appendix III for the proof)

$$P_{\text{out,m}}^{\text{lb},\infty} = \left[\sum_{j=1}^{M-1}\Omega_{\text{lb},m}^{(j)}\right]\left(\frac{\gamma_{th}}{\bar{\gamma}_{S,R}}\right)^{G_{d,m}^{\text{lb}}} + o\left(\bar{\gamma}_{S,R}^{-(G_{d,m}^{\text{lb}}+1)}\right), \tag{19}$$

where the lower bound of the diversity order is given by

$$G_{d,m}^{\mathrm{lb}} = N_m - N_R + 1. \tag{20}$$

In (19), the system dependent constant, $\Omega_{\mathrm{lb,m}}^{(j)}$, is given by

$$\Omega_{\mathrm{lb,m}}^{(j)} = \frac{\left(\phi_m^{(j)}\right)^{N_m-N_R+1}}{\Gamma(N_m-N_R+2)\beta^{N_m-N_R+1}}, \tag{21}$$

where $\bar{\gamma}_{m,R} = \bar{\gamma}_{S,R}$, $\bar{\gamma}_{R,m} = \bar{\gamma}_{R,S}$, $\bar{\gamma}_{R,S} = \beta\bar{\gamma}_{S,R}$, $\phi_m^{(j)} = \frac{\mathcal{T}_n(\mathcal{T}_j+\mathcal{T}_{j+1})}{\mathcal{T}_j}$, and $\phi_m^{(j)} = \frac{\mathcal{T}_n(\mathcal{T}_j+\mathcal{T}_{j+1})}{\mathcal{T}_{j+1}}$ for $m \in \{1,\cdots,M\}$, $j \in \{1,\cdots,M-1\}$ and $n \in \{1,\cdots,M-1\}$.

Now, the high SNR approximation for the lower bound of the overall outage probability is derived as

$$P_{\mathrm{out}}^{\mathrm{lb},\infty} = \left[\sum_{m'}\sum_{j=1}^{M-1}\Omega_{\mathrm{lb},m'}^{(j)}\right]\left(\frac{\gamma_{th}}{\bar{\gamma}_{S,R}}\right)^{G_d^{\mathrm{lb}}} + o\left(\bar{\gamma}_{S,R}^{-(G_d^{\mathrm{lb}}+1)}\right), \tag{22}$$

where $m' \in \{m' | G_{d,m'}^{\mathrm{lb}} = \min(N_1,\cdots,N_{m'},\cdots,N_M) - N_R + 1\}$. Moreover, the lower bound of the overall diversity order is given by

$$G_d^{\mathrm{lb}} = \min_{m\in\{1,\cdots,M\}}(N_m) - N_R + 1. \tag{23}$$

2) High SNR approximation of the upper bound of P_{out}: First, the high SNR approximation for the upper bound of the outage probability of mth source is derived by employing similar techniques to those in Appendix III and [3] as follows:

$$P_{\mathrm{out,m}}^{\mathrm{ub},\infty} = \left[\sum_{j=1}^{M-1}\Omega_{\mathrm{ub},m}^{(j)}\right]\left(\frac{\gamma_{th}}{\bar{\gamma}_{S,R}}\right)^{G_{d,m}^{\mathrm{ub}}} + o\left(\bar{\gamma}_{S,R}^{-(G_{d,m}^{\mathrm{ub}}+1)}\right), \tag{24}$$

where the upper bound of the diversity order is given by

$$G_{d,m}^{\mathrm{ub}} = N_m - N_R + 1. \tag{25}$$

In (24), the system dependent constant, $\Omega_{\mathrm{ub,m}}^{(j)}$, is given by

$$\Omega_{\mathrm{ub,m}}^{(j)} = \frac{\nu_m\left(\phi_m^{(j)}\right)^{N_m-N_R+1}}{(N_m-N_R+1)\beta^{N_m-N_R+1}}, \tag{26}$$

where $\phi_m^{(j)}$ and β are defined in (21). Moreover, in (26), ν_m is given by

$$\nu_m = \begin{cases} \frac{\det(\mathbf{\Psi}_m)}{(N_m-N_R+1)\prod_{l=1}^{N_R}[\Gamma(N_m-l+1)\Gamma(N_R-l+1)]}, & N_R \neq 1 \\ 1, & N_R = 1, \end{cases} \tag{27}$$

where $\mathbf{\Psi}_m$ for $m \in \{1,\cdots,M\}$ is an $(N_R-1)\times(N_R-1)$ matrix, where the (u,v)th element is given by $[\mathbf{\Psi}_m]_{u,v} = \Gamma(N_m - N_R + u + v + 1)$.

Next, the high SNR approximation for the upper bound of the overall outage probability can be derived as

$$P_{\mathrm{out}}^{\mathrm{ub},\infty} = \left[\sum_{m'}\sum_{j=1}^{M-1}\Omega_{\mathrm{ub},m'}^{(j)}\right]\left(\frac{\gamma_{th}}{\bar{\gamma}_{S,R}}\right)^{G_d^{\mathrm{ub}}} + o\left(\bar{\gamma}_{S,R}^{-(G_d^{\mathrm{ub}}+1)}\right), \tag{28}$$

Again, the index m' is same as in (24). Furthermore, in (28), G_d^{ub} is the upper bound of the overall diversity order, and is given by

$$G_d^{\mathrm{ub}} = \min_{m\in\{1,\cdots,M\}}(N_m) - N_R + 1. \tag{29}$$

Remark III.1: The lower and upper bounds of the diversity orders in (29) and (23), respectively, are the same, and consequently, the overall diversity order of the MIMO AF MWRN is given by $G_d = \min_{m\in\{1,\cdots,M\}}(N_m) - N_R + 1$.

D. Diversity-multiplexing trade-off

In this subsection, the fundamental DMT [11] of MIMO AF MWRNs with pair-wise transmit/receive ZF is derived to obtain valuable insights into practical system designing. In this system set-up, M independent symbol vectors each having N_R independent symbols are exchanged among M users in $2(M-1)$ time-slots. In this context, the effective mutual information can be upper bounded as

$$\mathcal{I}_{\mathrm{eff}} \lesssim \frac{MN_R}{2(M-1)}\log\left(1 + \min_{m\in\{1,\cdots,M\}}\gamma_{S_m,\min}^{\mathrm{ub}}\right). \tag{30}$$

Consequently, the information rate outage probability can be lower bounded as

$$\begin{aligned} P_{\mathrm{out}} &\lesssim \Pr(\mathcal{I}_{\mathrm{eff}} \leq \mathcal{R}_{th}) \\ &= \Pr\left(\min_{m\in\{1,\cdots,M\}}\gamma_{S_m,\min}^{\mathrm{ub}} \leq 2^{\frac{2(M-1)\mathcal{R}_{th}}{MN_R}} - 1\right), \end{aligned} \tag{31}$$

where $\mathcal{R}_{th}$ is the overall target information rate, and is defined a $\mathcal{R}_{th} = r\log(1+\bar{\gamma}_{S,R})$ [11]. By employing (22), P_{out} can be lower bounded when $\bar{\gamma}_{S,R} \to \infty$ as

$$P_{\mathrm{out}}^{\bar{\gamma}_{S,R}\to\infty} \gtrsim \bar{\gamma}_{S,R}^{-\left(\min_{m\in\{1,\cdots,M\}}(N_m)-N_R+1\right)\left(1-\frac{2r(M-1)}{MN_R}\right)}. \tag{32}$$

The effective mutual information can be lower bounded as

$$\mathcal{I}_{\mathrm{eff}} \gtrsim \frac{MN_R}{2(M-1)}\log\left(1 + \min_{m\in\{1,\cdots,M\}}\gamma_{S_m,\min}^{\mathrm{lb}}\right). \tag{33}$$

Now, by using similar steps to those in (31), (32), and then employing (28), P_{out} can be upper bounded $\bar{\gamma}_{S,R} \to \infty$ as

$$P_{\mathrm{out}}^{\bar{\gamma}_{S,R}\to\infty} \lesssim \bar{\gamma}_{S,R}^{-\left(\min_{m\in\{1,\cdots,M\}}(N_m)-N_R+1\right)\left(1-\frac{2r(M-1)}{MN_R}\right)}. \tag{34}$$

In particular, the lower and upper bounds of P_{out} in (32) and, (34), respectively, coincide and hence the achievable DMT can be derived as [11]

$$G_d(r) = \left(\min_{m\in\{1,\cdots,M\}}(N_m) - N_R + 1\right)\left(1 - \frac{2r(M-1)}{MN_R}\right). \tag{35}$$

It is worth noticing that the achievable diversity order reduces as the number of antennas at the relay (N_R) increase; however, the achievable multiplexing gain increases. The maximum achievable diversity order and multiplexing gain are given by $G_d = \min_{m\in\{1,\cdots,M\}}(N_m) - N_R + 1$, and $r = \frac{MN_R}{2(M-1)}$, respectively. Interestingly, r is maximized when $M = 2$, i.e., $r_{\max} = \lim_{M\to 2}\frac{MN_R}{2(M-1)} = N_R$. However, for large M, r approaches $N_R/2$, i.e., $r_{\min} = \lim_{M\to\infty}\frac{MN_R}{2(M-1)} = \frac{N_R}{2}$.

IV. Numerical Results

In Fig. 1, the overall outage probability of a MIMO four-way AF relay network is plotted for several antenna set-ups. Specifically, the exact outage probability is plotted by using Monte-Carlo simulation results, and the lower and upper bounds are plotted by employing (16), and (18), respectively. Moreover, asymptotic outage bounds are also plotted by using (22), and (28) to compare the achievable diversity orders. Fig. 1 clearly reveals that the outage probability improves significantly as the number of antennas at the relay decreases. For instance, at 10^{-4} outage probability, single-antenna relay results in a 6 dB SNR gain over the dual-antenna relay. However, the single-antenna set-up achieves this outage gain over

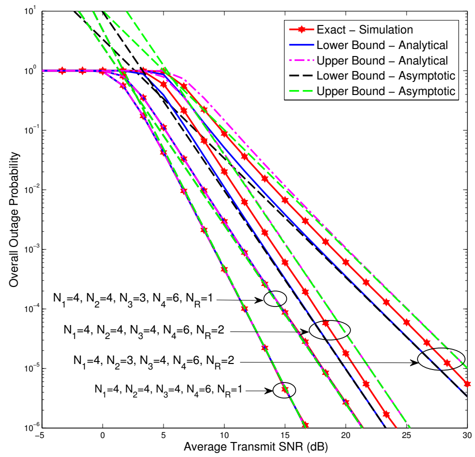

Fig. 1. The overall outage probability for the SNR threshold $\gamma_{th} = 5.00\,\text{dB}$.

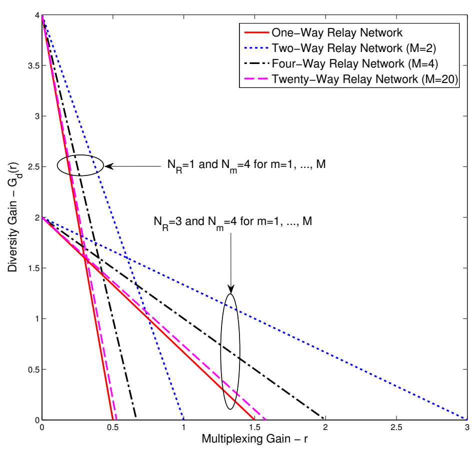

Fig. 2. The DMT of MIMO AF MWRNs with pair-wise ZF transmission.

the latter at the expense of a significant spatial multiplexing loss as quantified in (35). In particular, for single-antenna relays, our outage bounds reduce to exact outage as $N_R = 1$ case results in a unit-rank Wishart matrix, $\mathbf{H}_{R,i}^H \mathbf{H}_{R,i}$.

In Fig. 2, the achievable DMT curves are plotted for several system set-ups. Specifically, the DMT of the MIMO AF OWRN serves as a benchmark to compare the performance of MWRNs. The achievable multiplexing gain is improved as the number of relay antennas increases. However, at the same time, higher number of relay antennas significantly reduces the achievable diversity gains. Interestingly, TWRN provides the highest multiplexing gain for a given N_R. However, as the number of sources increases, the achievable spatial multiplexing gain gradually decreases to $N_R/2$, which is exactly the same multiplexing gain achieved by the OWRN. Thus, the MIMO AF MWRNs with pair-wise ZF transmission exhibit diminishing multiplexing gains as the network size grows.

V. Conclusion

The performance of the MIMO AF MWRNs with pair-wise Tx/Rx ZF transmission was studied over Rayleigh fading. To this end, the lower and upper bounds of the overall outage probability were derived in closed-form. Moreover, high SNR outage probability approximations were derived, and thereby achievable DMT was quantified to obtain valuable insights into practical MIMO MWRN system-designing. Interestingly, our outage probability bounds reduce to exact outage probability for single-antenna relays, and hence, they serve as benchmarks for practical MIMO AF MWRNs. Furthermore, the pair-wise transmit/receive ZF strategy requires each source to know only its channel to the relay, and consequently, eliminates the requirement of the global CSI for each source. Our DMT analysis reveals that increasing the number of relay antennas reduces the diversity gains, however improves the multiplexing gains. Counter intuitively, it is also shown that this multiplexing gain gradually diminishes as the number of participating sources linearly grows.

Appendix I: Proof of $P_{\text{out,m}}^{\text{lb}}$

In this Appendix, the lower bound of the outage probability of the mth source is sketched. To this end, the maximum diagonal element of the inverse of a Wishart matrix can be lower bounded by its arbitrary ath diagonal element as [3]

$$\max_{k\in\{1\cdots N_R\}}\left[\left(\left(\mathbf{H}_{R,m}^{(j)}\right)^H \mathbf{H}_{R,m}^{(j)}\right)^{-1}\right]_{k,k} \geq \left[\left(\left(\mathbf{H}_{R,m}^{(j)}\right)^H \mathbf{H}_{R,m}^{(j)}\right)^{-1}\right]_{a,a}, \quad (36)$$

where $a \in \{1, \cdots, N_R\}$. Next, the smallest post-processing subchannel SNR of S_m received in the jth time-slot of the BC phase can be upper bounded as

$$\min_{k\in\{1\cdots N_R\}}\left[\gamma_{S_m^{(j)}}\right]_k \leq \gamma_{S_{m,\min}}^{(j),\text{ub}} = \frac{\eta_m^{(j)}}{\zeta_m^{(j)} + \mu_m^{(j)}\left[\left(\left(\mathbf{H}_{R,m}^{(j)}\right)^H \mathbf{H}_{R,m}^{(j)}\right)^{-1}\right]_{a,a}}, \quad (37)$$

where $\mu_m^{(j)}$, $\eta_m^{(j)}$, and $\zeta_m^{(j)}$ are defined in (10). By substituting (37) into (8), $P_{\text{out,m}}$ can be lower bounded as

$$P_{\text{out,m}} \geq P_{\text{out,m}}^{\text{lb}} = \Pr\left(\min_{j\in\{1,\cdots,M-1\}} \gamma_{S_{m,\min}}^{(j),\text{ub}} \leq \gamma_{th}\right). \quad (38)$$

In order to derive $P_{\text{out,m}}^{\text{lb}}$ in closed-form, the CDF of $\gamma_{S_{m,\min}}^{(j),\text{ub}}$ is obtained as follows:

$$F_{\gamma_{S_{m,\min}}^{(j),\text{ub}}}(x) = 1 - \Pr\left(X_m^{(j)} \leq \frac{\eta_m^{(j)} - \zeta_m^{(j)} x}{\mu_m^{(j)} x}\right), \quad (39)$$

where $X_m^{(j)} = \left[\left(\left(\mathbf{H}_{R,m}^{(j)}\right)^H \mathbf{H}_{R,m}^{(j)}\right)^{-1}\right]_{a,a}$. For $x \geq \eta_m^{(j)}/\zeta_m^{(j)}$, $F_{\gamma_{S_{m,\min}}^{(j),\text{ub}}}(x) = 1$, and for $x < \eta_m^{(j)}/\zeta_m^{(j)}$, $F_{\gamma_{S_{m,\min}}^{(j),\text{ub}}}(x)$ becomes

$$F_{\gamma_{S_{m,\min}}^{(j),\text{ub}}}(x) = 1 - \int_0^{\frac{\eta_m^{(j)} - \zeta_m^{(j)} x}{\mu_m^{(j)} x}} f_{X_m^{(j)}}(y)\,\mathrm{d}y, \quad (40)$$

where $f_{X_m^{(j)}}(x)$ can be obtained by substituting the PDF of $1/X_m^{(j)}$, which is given by $f_{1/X_m^{(j)}}(x) = \frac{x^{N_m - N_R} \mathrm{e}^{-x}}{\Gamma(N_m - N_R + 1)}$ [13] into the transformation $f_{X_m^{(j)}}(x) = \frac{1}{x^2} f_{1/X_m^{(j)}}(1/x)$ as follows:

$$f_{X_m^{(j)}}(x) = \frac{\mathrm{e}^{-1/x}}{\Gamma(N_m - N_R + 1) x^{N_m - N_R + 2}}. \quad (41)$$

Next, by substituting (41) into (40), and by applying a change of variable, $y = 1/t$, (40) can be rearranged as

$$F_{\gamma^{(j),\mathrm{ub}}_{S_m,\min}}(x) = 1 - \int_{\frac{\mu_m^{(j)} x}{\eta_m^{(j)} - \zeta_m^{(j)} x}}^{\infty} \frac{t^{N_m - N_R} \mathrm{e}^{-t}}{\Gamma(N_m - N_R + 1)} \mathrm{d}t. \quad (42)$$

By using [14, Eq. (8.350.2)], (42) can now be evaluated in closed-form as in (10). By substituting (42) into the CDF of minimum of $M-1$ independent random variables, the desired results can be derived as in (9).

APPENDIX II :PROOF OF $P_{\mathrm{out,m}}^{\mathrm{ub}}$

In this Appendix, the outage upper bound of the mth source is derived. To this context, the maximum diagonal element of the inverse of a Wishart matrix is upper bounded as [9]

$$\max_{k\in\{1\cdots N_R\}} \left[\left(\left(\mathbf{H}_{R,i}^{(j)}\right)^H \mathbf{H}_{R,i}^{(j)} \right)^{-1} \right]_{k,k} \leq \lambda_{\min}^{-1} \left(\left(\mathbf{H}_{R,i}^{(j)}\right)^H \mathbf{H}_{R,i}^{(j)} \right). \quad (43)$$

The smallest subchannel SNR of S_m received in the jth time-slot of the BC phase can then be lower bounded by substituting (43) into (7) as follows:

$$\min_{k\in\{1\cdots N_R\}} \left[\gamma_{S_m^{(j)}} \right]_k \geq \gamma^{(j),\mathrm{lb}}_{S_m,\min} = \frac{\eta_m^{(j)}}{\zeta_m^{(j)} + \mu_m^{(j)} \lambda_{\min}^{-1} \left(\left(\mathbf{H}_{R,i}^{(j)}\right)^H \mathbf{H}_{R,i}^{(j)} \right)}, \quad (44)$$

where $\mu_m^{(j)}$, $\eta_m^{(j)}$, and $\zeta_m^{(j)}$ are defined in (10). By substituting (44) into (8), $P_{\mathrm{out,m}}$ can now be upper bounded as

$$P_{\mathrm{out,m}} \leq P_{\mathrm{out,m}}^{\mathrm{ub}} = \Pr\left(\min_{j\in\{1,\cdots,M-1\}} \gamma^{(j),\mathrm{lb}}_{S_m,\min} \leq \gamma_{th} \right). \quad (45)$$

Next, by using similar steps to those in [3], the CDF of $\gamma^{(j),\mathrm{lb}}_{S_m,\min}$ can be derived as in (12) to obtain the desired result.

APPENDIX III :PROOF OF $P_{\mathrm{out}}^{\mathrm{lb},\infty}$

In this Appendix, the proof of the lower bound for the diversity order is sketched. To begin with, the PDF of $\gamma^{(j),\mathrm{ub}}_{S_m,\min}$ for $j \in \{1, \cdots, M-1\}$ is derived by differentiating (9) with respect to variable x by using the Leibniz integral rule as follows:

$$f_{\gamma^{(j),\mathrm{ub}}_{S_m,\min}}(x) = \frac{\eta_m^{(j)} \left(\mu_m^{(j)}\right)^{N_m - N_R + 1} x^{N_m - N_R} \, \mathrm{e}^{\frac{-\mu_m^{(j)} x}{\eta_m^{(j)} - \zeta_m^{(j)} x}}}{\Gamma(N_m - N_R + 1) \left(\eta_m^{(j)} - \zeta_m^{(j)} x \right)^{N_m - N_R + 2}}, \quad (46)$$

where $0 \leq x < \frac{\eta_m^{(j)}}{\zeta_m^{(j)}}$. By substituting $\mu_m^{(j)}$, $\eta_m^{(j)}$, and $\zeta_m^{(j)}$, defined in (10) into (46), and then by taking the Taylor series expansion around $x = 0$, the first order expansion[10] of $f_{\gamma^{(j),\mathrm{ub}}_{S_m,\min}}(x)$ when $\lim_{x\to 0}$ can be derived as

$$f^{x\to 0}_{\gamma^{(j),\mathrm{ub}}_{S_m,\min}}(x) = \frac{\left(\phi_m^{(j)}\right)^{N_m - N_R + 1} x^{N_m - N_R}}{(N_m - N_R)! \, (\beta \bar{\gamma}_{SR})^{N_m - N_R + 1}} + o\left(x^{N_m - N_R + 1}\right). \quad (47)$$

[10]The first order expansion of $f(x)$ is the single-term polynomial approximation of $f(x)$ consisting with the lowest power of x [15].

The first order expansion of the CDF of $\gamma^{(j),\mathrm{ub}}_{S_m,\min}$ when $\lim_{x\to 0}$ can be derived by using (47) as [15]

$$F^{x\to 0}_{\gamma^{(j),\mathrm{ub}}_{S_m,\min}}(x) = \Omega^{(j)}_{\mathrm{lb},m} \left(\frac{\gamma_{th}}{\bar{\gamma}_{S,R}} \right)^{G^{\mathrm{lb}}_{d,m}} + o\left(\bar{\gamma}_{S,R}^{-(G^{\mathrm{lb}}_{d,m}+1)} \right), \quad (48)$$

where $G^{\mathrm{lb}}_{d,m}$ and $\Omega^{(j)}_{\mathrm{lb},m}$ are defined in (20) and (21). Next, the first order expansion of the CDF of $Y_m = \min_{j\in\{1,\cdots,M-1\}} \left(\gamma^{(j),\mathrm{lb}}_{S_m,\min}\right)$ can be derived by using substituting (48) into $F_{Y_m}(x) = 1 - \prod_{j=1}^{M-1} \left(1 - F_{\gamma^{(j),\mathrm{ub}}_{S_m,\min}}(x)\right)$ and by using the identity, $\prod_{l=1}^{L}(1 - y_l) = 1 + \sum_{l=1}^{L}(-1)^l \sum_{\lambda_1=1}^{L-l+1} \sum_{\lambda_2=\lambda_1+1}^{L-l+2} \cdots\cdots \sum_{\lambda_l=\lambda_{l-1}}^{L} \prod_{n=1}^{l} y_{\lambda_n}$, as follows:

$$F_{Y_m^{\infty}}(x) = \left[\sum_{j=1}^{M-1} \Omega^{(j)}_{\mathrm{lb},m} \right] \left(\frac{x}{\bar{\gamma}_{S,R}} \right)^{G^{(j),\mathrm{lb}}_{d,m}} + o\left(x^{(G^{(j),\mathrm{lb}}_{d,m}+1)} \right). \quad (49)$$

Next, by using a similar technique, the first order expansion of the CDF of $Z = \min_{j\in\{1,\cdots,M-1\}} (Y_m)$ can be derived by substituting (49) into the expansion of $F_Z(x) = 1 - \prod_{m=1}^{M} \left(1 - F_{Y_m^{\infty}}(x)\right)$ to obtain the desired result in (22).

REFERENCES

[1] B. Rankov and A. Wittneben, "Spectral efficient protocols for half-duplex fading relay channels," *IEEE J. Sel. Areas Commun.*, vol. 25, no. 2, pp. 379–389, Feb. 2007.

[2] R. Zhang *et al.*, "Optimal beamforming for two-way multi-antenna relay channel with analogue network coding," *IEEE J. Sel. Areas Commun.*, vol. 27, no. 5, pp. 699–712, Jun. 2009.

[3] G. Amarasuriya, C. Tellambura, and M. Ardakani, "Performance analysis of zero-forcing for two-way MIMO AF relay networks," *IEEE Wireless Commun. Lett.*, vol. 1, no. 2, pp. 53–56, Apr. 2012.

[4] E. van der Meulen, "A survey of multi-way channels in information theory: 1961-1976," *IEEE Trans. Inf. Theory*, vol. 23, no. 1, pp. 1–37, Jan. 1977.

[5] D. Gunduz *et al.*, "The multi-way relay channel," in *Proc. IEEE Int. Sympo. on Info. Theory., (ISIT)*, Jul. 2009, pp. 339–343.

[6] A. Amah and A. Klein, "Non-regenerative multi-way relaying with linear beamforming," in *Proc. IEEE Personal, Indoor and Mobile Radio Commun., (PIMRC)*, Sep. 2009, pp. 1843–1847.

[7] Z. Zhao *et al.*, "A special case of multi-way relay channel: When beamforming is not applicable," *IEEE Trans. Wireless Commun.*, vol. 10, no. 7, pp. 2046–2051, Jul. 2011.

[8] L. Ong, S. Johnson, and C. Kellett, "An optimal coding strategy for the binary multi-way relay channel," *IEEE Commun. Lett.*, vol. 14, no. 4, pp. 330–332, Apr. 2010.

[9] J. Heath, R.W., S. Sandhu, and A. Paulraj, "Antenna selection for spatial multiplexing systems with linear receivers," *IEEE Commun. Lett.*, vol. 5, no. 4, pp. 142–144, Apr. 2001.

[10] R. Louie, Y. Li, and B. Vucetic, "Zero forcing in general two-hop relay networks," *IEEE Trans. Veh. Technol.*, vol. 59, no. 1, Jan. 2010.

[11] D. N. C. Tse, P. Viswanath, and L. Zheng, "Diversity-multiplexing tradeoff in multiple-access channels," *IEEE Trans. Inf. Theory*, vol. 50, no. 9, pp. 1859–1874, Sep. 2004.

[12] L. G. Ordóñez, "Performance limits of spatial multiplexing MIMO systems," Ph.D. dissertation, Technical University of Catalonia (UPC), Barcelona, Spain, Mar. 2009.

[13] D. Gore, J. Heath, R.W., and A. Paulraj, "On performance of the zero forcing receiver in presence of transmit correlation," in *Proc. IEEE Int. Sympo. on Inf. Theory (ISIT)*, Lausanne, Switzerland, Jul. 2002, pp. 1–2.

[14] I. Gradshteyn and I. Ryzhik, *Table of integrals, Series, and Products*, 7th ed. Academic Press, 2007.

[15] Z. Wang and G. B. Giannakis, "A simple and general parameterization quantifying performance in fading channels," *IEEE Trans. Commun.*, vol. 51, no. 8, pp. 1389–1398, Aug. 2003.